

See discussions, stats, and author profiles for this publication at: <https://www.researchgate.net/publication/328405055>

# Sedimentation rate of soil microparticles

Article in *Arabian Journal of Geosciences* · October 2018

DOI: 10.1007/s12517-018-4002-8

CITATION

1

READS

239

6 authors, including:



**Milan Gombos**

Slovak Academy of Sciences

26 PUBLICATIONS 40 CITATIONS

[SEE PROFILE](#)



**Andrej Tall**

Slovak Academy of Sciences

15 PUBLICATIONS 11 CITATIONS

[SEE PROFILE](#)



**Jarmila Trpčevská**

Technical University

52 PUBLICATIONS 128 CITATIONS

[SEE PROFILE](#)



**Branislav Kandra**

Slovak Academy of Sciences

16 PUBLICATIONS 16 CITATIONS

[SEE PROFILE](#)

Some of the authors of this publication are also working on these related projects:



Processing of industrial wastes with the aim to obtain zinc, tin and lead - based marketable products [View project](#)



Hard zinc processing, production of alloys from zinc drosses [View project](#)



# Sedimentation rate of soil microparticles

Milan Gomboš<sup>1</sup> · Andrej Tall<sup>1</sup> · Jarmila Trpčevská<sup>2</sup> · Branislav Kandra<sup>1</sup> · Dana Pavelkova<sup>1</sup> · Lucia Balejčíková<sup>1</sup>

Received: 12 March 2018 / Accepted: 12 October 2018  
© Saudi Society for Geosciences 2018

## Abstract

The aim of the submitted paper is to identify the lower limit of Stokes' law for calculating the deposition rate of soil microparticles. The authors' hypothesis on the lower limit of Stokes' law is based on the idea that with the gradual formation of the colloidal dispersion system, both the particle size and the sedimentation rate decrease. It is assumed that under the lower particle size limit, Stokes' law does not apply. As a result of the diffusion, the state of the sedimentation equilibrium gradually emerges. The results of the experiment showed that in laboratory conditions, Stokes' equation ceases to be valid for sedimentation of the particles sized  $d(90) < 2 \mu\text{m}$ . During the experiment, a dynamic sedimentation equilibrium was reached at the particle size  $d(90) = 0.27 \mu\text{m}$ . The scientific contribution of this knowledge is the accuracy of the determination of hydrogeological characteristics dependent on the texture of the soil. In this context, the results stated in the paper define the lower limit of the validity for the laboratory procedures determining soil texture on the basis of the sedimentation methods. To identify the textures below this limit, it is necessary to choose the methods based on other principles. Determination of the lower limit is particularly important in clay soils containing a high proportion of clay particles (clay particles  $< 2 \mu\text{m}$ ).

**Keywords** Soil microparticles · Disperse system · Sedimentation rate

## Introduction

The deposition rate of soil microparticles has not been solved. Soil microparticles (particle size app.  $1\text{E}-6 \text{ m}$ ) are formed by clay particles with high content of clay minerals. Soils with high content of clay particles ( $> 35\%$ ) are known as clayey soils (<http://www.fao.org>). Clay particles are defined as particles with the size  $\leq 2 \mu\text{m}$  containing clay minerals. As hydraulics considers a moving object in a fluid and a stationary object in a moving fluid equivalent, the movement of microparticles in water was examined by means of the sedimentation analysis (Allain et al. 1995; Durner et al. 2017; McRoberts and Nixon 1976; Paul et al. 2017; Piazza 2014; Richter and Nikrityuk 2013; Rong et al. 2015; Tan et al. 1990; Zhang et al., 2013, 2017). The sedimentation analysis is based on Stokes' law, which is also referred to as the relation

for sedimentation rate. It was derived in 1851 by Irish mathematician and physicist George Gabriel Stokes. It is assumed that moving particles are much larger than water molecules; they have the shape of spheres and move at low speeds in the laminar flow region. Hydrological and hydrogeological research and investigation include the acquisition of hydrogeological characteristics of the soil environment. The obtained hydrogeological characteristics are one of the inputs into mathematical numerical models designed to simulate hydrological processes in the soil environment. The quality of inputs used in the models significantly affects the quality and representativeness of outputs from numerical simulations. Hydrogeological characteristics depend on the texture of the porous environment. They are obtained from fieldwork and laboratory measurements. Laboratory procedures for texture identification are based on the sedimentation methods based on Stokes' law. These are still used by default. Problems arise when quantitating clay particles. These do not meet the condition of size and shape. For this reason, it is necessary to know the lower limit of Stokes' law, under which the methods based on other principles must be chosen. The sedimentation analysis was performed by the fractionation of a soil suspension containing particles with the size  $\leq 10 \mu\text{m}$ , which formed a colloidal dispersion—lyosol—composed of clay particles in water (Bartovská and Šišková 2010; Everett 1988; Guan et al.

✉ Dana Pavelkova  
pavelkova@uh.savba.sk

<sup>1</sup> Institute of Hydrology, Slovak Academy of Sciences in Bratislava, Dúbravská cesta 9, 841 04 Bratislava, Slovakia

<sup>2</sup> Faculty of Materials, Metallurgy and Recycling of the Technical University of Košice, Letná 9, 042 00 Košice, Slovakia

2017; Arkhipov et al. 2016; Dellino et al. 2018). The aim of the analysis was to measure the sedimentation rate of different fractions of soil microparticles created during the sedimentation and to define the lower validity limit for Stokes' equation. The morphology of the examined soil microparticles was analysed under a scanning electron microscope. For the sedimentation experiment, the location in East Slovak Lowland (ESL), which lies in the eastern part of the Slovak Republic, was selected. The ESL genetically represents the most northerly part of the extensive intra-Carpathian tectonic depression of the East Slovakian basin. It was caused by uneven tectonic drops of the Earth's crust within the Carpathian Arc during the Neogen and Quaternary. Decreasing movements caused the prevalence of accumulation processes and thus formed the flat low surface. The soil characteristics in the ESL correspond to the geological development of the area in terms of typology and species. The typical soils of the area are clay soils, which form 42% of the total ESL soils. The genetic properties of soils on ESL are differentiated by the formation of geomorphic complexes. Up to 59% of soils were formed under hydromorphological and alluvial conditions. Fluvial and glue soils with unfavourable physical and physicochemical properties were mainly developed.

## Materials and methods

### Theory of sedimentation

The sedimentation rate of particles in a disperse system depends on forces acting on the particles. In gravitational field, a settling particle in a fluid is under the influence of gravity  $F_g$  and the opposing forces, buoyancy  $F_b$  and drag force  $F_D$  (Haider and Levenspiel 1989; McRoberts and Nixon 1976; Piazza 2014; Zaidi et al. 2014). At the beginning of sedimentation, settling particles increase their speed. At a certain speed, the drag force increases to such an extent that the forces come into equilibrium. The sedimentation rate is constant if the forces are balanced:

$$F_D = F_g - F_b \quad (1)$$

Equation (1) can be expressed in the form

$$f \cdot u = V \cdot \rho \cdot g - V \cdot \rho_0 \cdot g \quad (2)$$

where  $f$  is the friction coefficient, which depends on the shape and size of particles,  $u$  is the sedimentation rate,  $V$  is the volume of a settling particle,  $\rho$  is the volumetric mass density of a settling particle,  $\rho_0$  is the volumetric mass density of a dispersion medium and  $g$  is the gravitational acceleration on the surface.

Furthermore, drag force is defined by the equation

$$F_D = C_D \cdot S \cdot \rho \cdot \frac{u^2}{2} \quad (3)$$

where  $C_D$  is the drag coefficient,  $S$  is the cross-sectional area of a particle and  $\rho \cdot \frac{u^2}{2}$  is the hydrodynamic pressure of laminar flow.

For spherical particles with the radius  $r$ , dispersed in a dispersion medium with the viscosity  $\eta_0$ , Stokes derived an equation for the friction coefficient  $f$  based on Navier-Stokes' equations (Stokes 1850):

$$f = 6 \cdot \pi \cdot \eta_0 \cdot r \quad (4)$$

from which the equation for drag force is

$$F_D = 6 \cdot \pi \cdot \eta_0 \cdot r \cdot u \quad (5)$$

and, subsequently, from Eqs. (5) and (3), the equation for drag coefficient  $C_D$  of a spherical particle is

$$C_D = \frac{24}{Re} \quad (6)$$

where  $Re = \frac{\rho \cdot d \cdot u}{\eta_0}$  is Reynolds' number.

The combination of Eqs. (2) and (4) gives Stokes' equation (7) describing the sedimentation rate of spherical particles:

$$u = \frac{2}{9} \frac{(\rho - \rho_0) \cdot r^2 \cdot g}{\eta_0} \quad (7)$$

The equations are valid for spherical particles which are bigger than the molecules of the surrounding environment, assuming that their surface is smooth without any electric charge and that their velocity is low, within the area of the laminar flow with small values of Reynolds number ( $Re < 0.5$ ) (Johnson and Patel 1999; Ouchene et al. 2015). When calculating the sedimentation rate of soil particles, the deviations from real conditions are caused by the fact that the assumptions of spherical particles and the size of particles are not met. If the particles are not spherical, the equation for Stokes' drag must be modified as follows:

$$F_{Dm} = f_e \cdot u = 3 \cdot \pi \cdot \eta_0 \cdot d_e \cdot u \cdot K \quad (8)$$

where  $d_e$  is the diameter of a sphere with the same volume as a non-spherical particle, i.e.

$$d_e = \left( \frac{6}{\pi} \times V \right)^{\frac{1}{3}} \quad (9)$$

and  $K$  is the correction factor which depends on the shape and size of a particle.

Because of this, the friction coefficient for simple non-spherical particles is assessed only theoretically. For instance,

for an ellipsoid of revolution, the friction coefficient for non-spherical particles is calculated as follows:

$$f_e = 3 \cdot \pi \cdot \eta_0 \cdot d_e \cdot \frac{a-b}{5 \cdot b} \tag{10}$$

where  $a, b$  are semi-major and semi-minor axes which can differ by a few orders of magnitude.

The sedimentation of particles in a disperse system occurs until dynamic (sedimentation) equilibrium of the system is reached.

In the experiment, one of the oldest methods of particle size analysis was used—sedimentation analysis. The disperse phase (i.e. soil particles) in the polydispersed system was statistically divided in the groups of particles of similar size called fractions. In the sedimentation analysis, the distribution of particles was expressed by means of the frequency and cumulative distribution functions.

The devices which work based on laser diffraction analysis measure the frequency of the particles of certain size in a disperse phase in percentage of the volume (Arriaga et al. 2006; Loizeau et al. 1994; Miller and Schaeztl 2012; Moshrefi 1993; Sperazza et al. 2004; Storti and Balsamo 2010; Taubner et al. 2009). Numerically, the value is the same as the value expressed as percentage of weight.

### Description of the experiment

The experimental site selected for the purposes of the sedimentation experiment is illustrated in Fig. 1. It is located in eastern Slovakia (N48° 39.802', E22° 02.892'). The area lies on the East Slovak Lowland (ESL) which is predominantly flat. The lowland is of tectonic origin with a complex structure of dip-slip faults, and it is formed mainly by Quaternary and Neogene sediments. The experimental site is located in the central part of the lowland, in the area called Senné depression with the altitude 100 m. Wetlands are a typical biotope of the area, thereof the creation of heavy soils in the area.

The soil in the sampling area is an extremely heavy soil predominantly composed of clay particles (more than 77% of the particles are smaller than 0.002 mm). Clay particles contain clay minerals, especially the minerals of montmorillonitic



Fig. 1 Location of the experimental site

and illitic groups, which cause volume changes at varying moisture levels. After being dried in the laboratory conditions, their volume change reaches up to 40% compared to the state of saturation (Gomboš et al. 2009). The content of silt particles in the soil is app. 18%. Sand is represented only minimally (~4%). The particle size distribution of the taken soil sample identified the sample within the USDA triangle as illustrated in Fig. 2. The sample was used to create the disperse phase.

At the next step of the analysis, a disperse system was created in which the settling of soil microparticles was observed. A solid disperse phase in a liquid dispersion medium (water) created a heterogeneous disperse system. At the beginning of the sedimentation, the disperse phase formed coarse dispersion  $d > 10^{-6}$  m. Subsequently, colloidal dispersion (lyosol) was formed which is defined for particles with the size from the interval  $10^{-9}$  m  $< d < 10^{-6}$  m. Taking into consideration the shape of the particles, the disperse system is supposed to be laminar with anisometric particles having the shape of a plate. From the viewpoint of particle sizes, the system is polydisperse, containing particles of different sizes.

The disperse system was prepared as follows: the soil sample was air-dried in the laboratory and then mechanically crushed. Afterwards, in order to remove soil skeleton, it was sieved through a sieve with the diameter of the mesh  $\varnothing$  2 mm; from the sifted mass, 0.4 kg of the soil was taken and put in a vessel together with distilled water and a dispersing agent. In this case, a solution of sodium hexametaphosphate ((NaPO<sub>3</sub>)<sub>6</sub>) and sodium carbonate (Na<sub>2</sub>CO<sub>3</sub>) in the ratio of 35.7:7.9 g for 1 l of distilled water. The created suspension was left still for 24 h. Then, it was boiled for 1 h while it was occasionally stirred. After it had been cooled, the suspension was poured into a sedimentation cylinder and replenished with distilled water to the volume of 5 l. The disperse system was

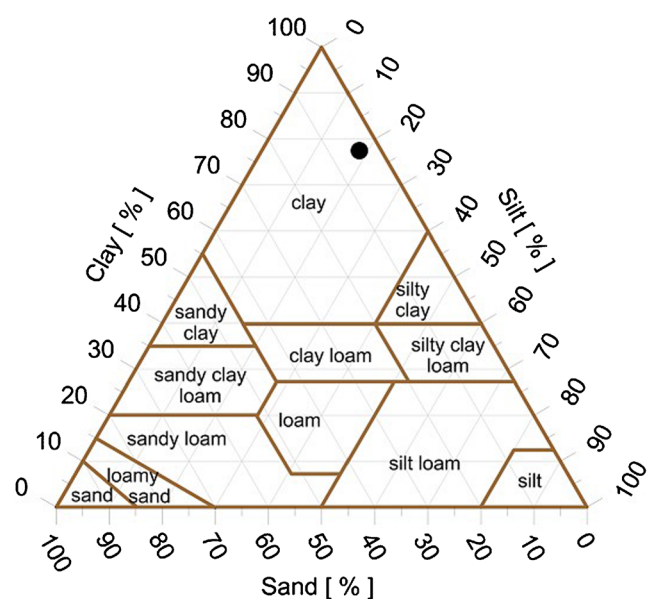


Fig. 2 Identification of the soil sample within the USDA triangle

then prepared for the experiment. The scheme of the experiment is illustrated in Fig. 3.

Particle size distribution of the samples was performed by laser diffraction. Laser diffraction measures particle size distribution by measuring the angular variation in the intensity of light scattered as a laser beam passes through a sample. Large particles scatter light at small angles relative to the laser beam, and small particles scatter light at large angles. The angular scattering intensity data is then analysed to calculate the size of the particles responsible for creating the scattering pattern, using the Mie theory of light scattering. The Mie theory requires the knowledge of the optical properties (refractive index and imaginary component) of the sample being measured, along with the refractive index of the dispersant. The particle size is reported as a volume equivalent sphere diameter.

Particle size distribution analysis was performed by the device Mastersizer 2000 (MALVERN Instruments) (Arriaga et al. 2006; Loizeau et al. 1994; Miller and Schaetzel 2012; Moshrefi 1993; Sperazza et al. 2004; Storti and Balsamo 2010). The device can be used for both dry and wet analysis. In this experiment, only wet analysis was used and it was performed by the dispersion unit Hydro 2000MU. Distilled water was used as a dispersion medium. Before performing the measurements, all samples were exposed to ultrasound for 5 min in order to gain better dispersing. The accuracy of measurements indicated by the manufacturer is between 0.02 and 2000  $\mu\text{m}$ .

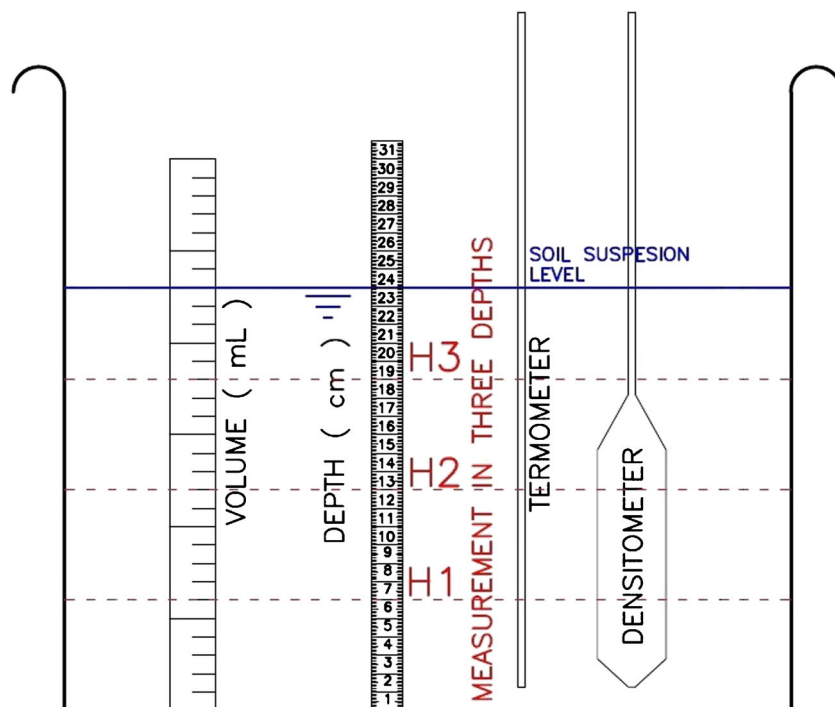
Before the start of the experiment, the suspension in the sedimentation cylinder was properly mixed so as to reach a homogeneous state. From that moment, the sedimentation process started to be counted. In the defined time intervals,

three samples of the suspension were taken by a pipette at three different heights from the bottom of the cylinder (6 cm, 12 cm and 18 cm). At the same time, the temperature (20 °C) and density of the suspension were monitored. Sampling time intervals were determined in a way that their growth was linear in a semi-logarithmic representation. Overall, 23 sets of samples were taken, comprising three samples each i.e. 69 samples in total. The experiment lasted for 42 days and 23 h. The sedimentation rate of a soil particle with the defined diameter can be calculated by measuring the time it passes a certain distance. The distance is defined by three sedimentation levels (6 cm, 12 cm and 18 cm above the bottom of the sedimentation cylinder). The time a particle passes the distance equals the delay between each sedimentation level. The sedimentation rates of soil particles were calculated based on values  $d(90)$ .

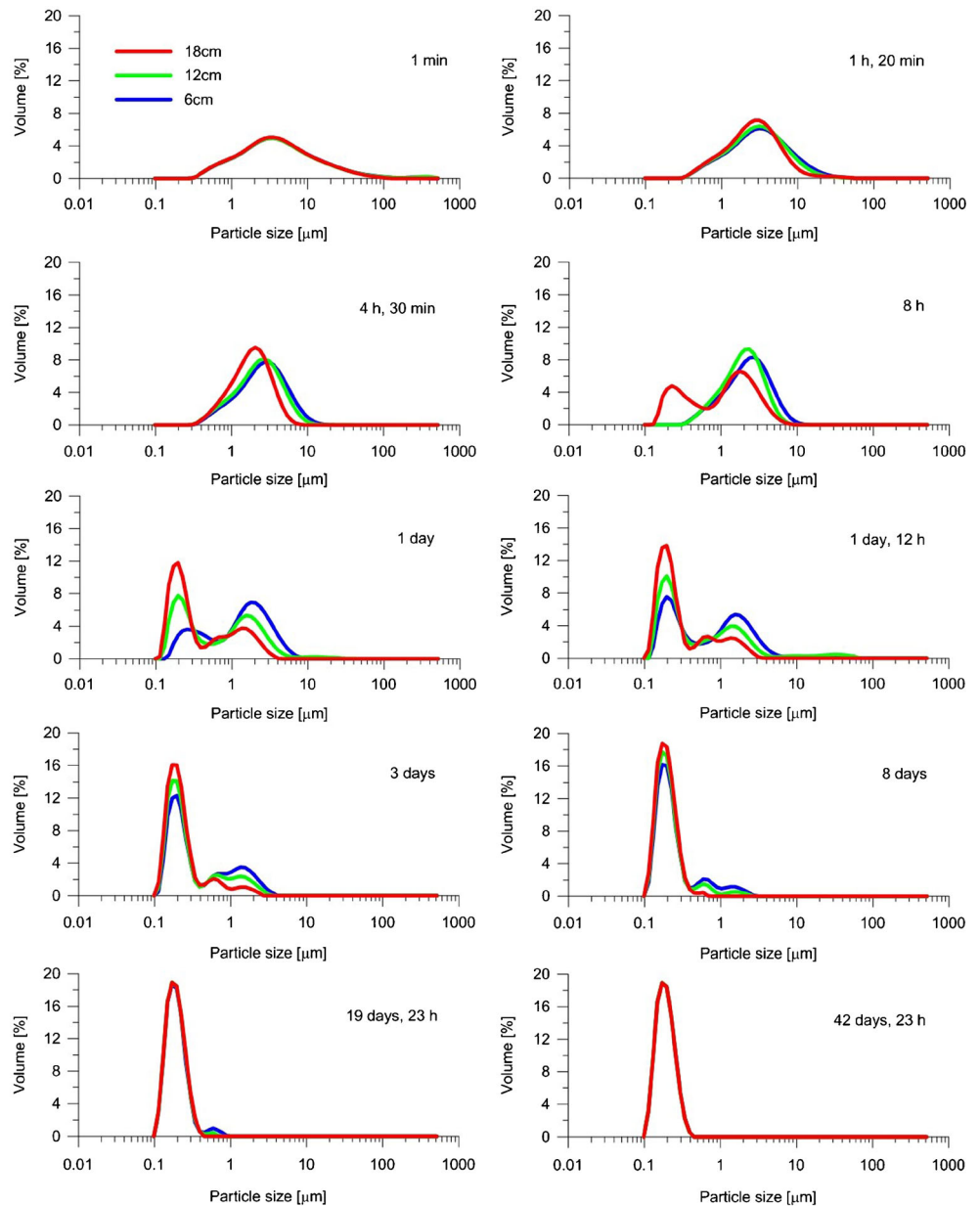
## Results

Figure 4 shows graphical outputs of the measurements performed by laser diffraction analysis at three levels, examining the textural structure of the heavy soil in question. The starting point of the measurements was the homogeneous state of the suspension in the zero time. At that moment, almost identical grain size distribution curves were identified at all three levels. Immediately after pulling the stirrer out of the cylinder, soil particles started to settle at different speeds, depending on their size. Soil particles in the suspension were sized from 550 to 0.1  $\mu\text{m}$ . Figure 4 shows the measured particle size

Fig. 3 Scheme of the experiment



**Fig. 4** Particle size distribution in the examined soil sample in ten selected time intervals



distribution of the examined soil in ten different time intervals. At the beginning of the experiment, the suspension was close to the homogeneous state, which was proven by the measurements—textural profiles at three monitored levels were very similar. From the beginning of the experiment up to 1 h and 20 min after the start of the experiment, the particle sizes prevailing at all three levels belonged in the interval 2.88–3.31 μm. After this time, prevailing particle sizes measured at the same time at different levels belonged in different size intervals. Prevailing particle sizes belonging in the same size interval were measured at different levels at different times. Subsequently, heterogeneity of the suspension gradually decreased. From day 7 of the experiment until its termination, prevailing particle sizes at all levels belonged in the same size interval again (0.16–0.18 μm). At the end of the experiment, grain size distribution

curves were almost identical at all three levels. In the created colloidal dispersion, the state of the sedimentation equilibrium was reached. The sedimentation rate of the dispersed particles in the state of dynamic equilibrium is equal to the diffusion rate in the opposite direction. In the state of the sedimentation equilibrium, particle sizes  $d$  on the distribution curve of particle sizes were identified in micrometers for  $d(10)$ ,  $d(50)$ , and  $d(90)$ . The values were obtained by the measurements by the laser analyser. In this case, the value  $d(90)$  is the maximum diameter of soil particles, which, at the time of the measurements, was present in the analysed suspension with 90% probability. For the indicated probabilities, the following particle sizes were identified:  $d(10) = 0.14 \mu\text{m}$ ,  $d(50) = 0.19 \mu\text{m}$  and  $d(90) = 0.27 \mu\text{m}$ . The smallest particle identified in the disperse system in the state of dynamic equilibrium was sized  $0.113 \mu\text{m}$ .

**Fig. 5** Prevailing particle sizes in respect of their diameter in the course of the experiment

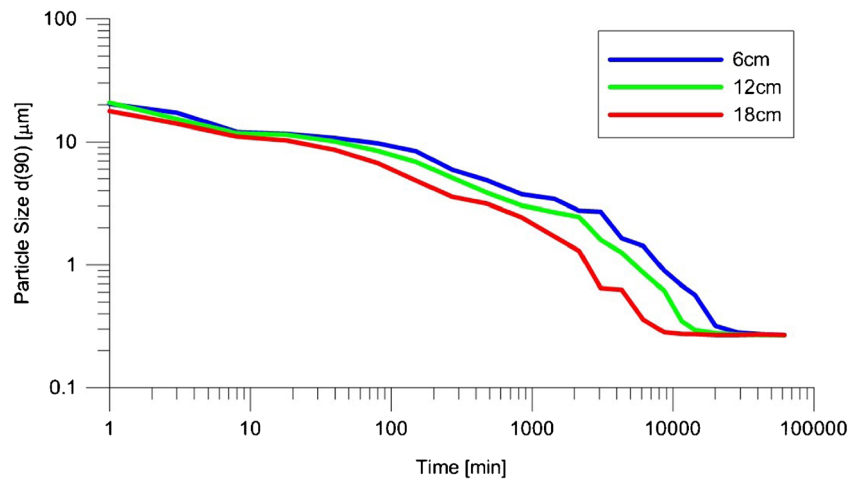
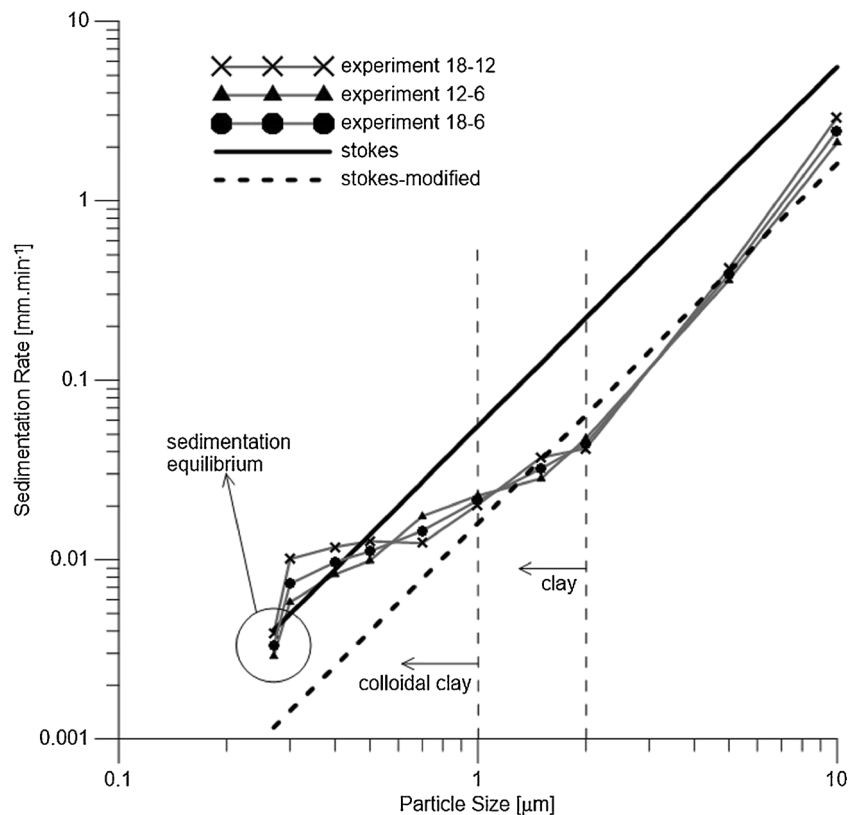


Figure 5 shows the development of the prevailing particle sizes at the selected levels in time in respect of their diameter. At the next step of the experiment, the sedimentation rates were calculated by Stokes' equation (7). Figure 6 shows the comparison between the calculated and the measured values. The comparison shows that the values calculated by Eq. (7) are bigger than the measured ones. In the interval of the particles sized  $\geq 2 \mu\text{m}$ , the trends of the calculated and the measured sedimentation rates are comparable. For particles sized  $< 2 \mu\text{m}$ , the measured sedimentation rates are significantly different from the linear function calculated by Stokes' equation. In the

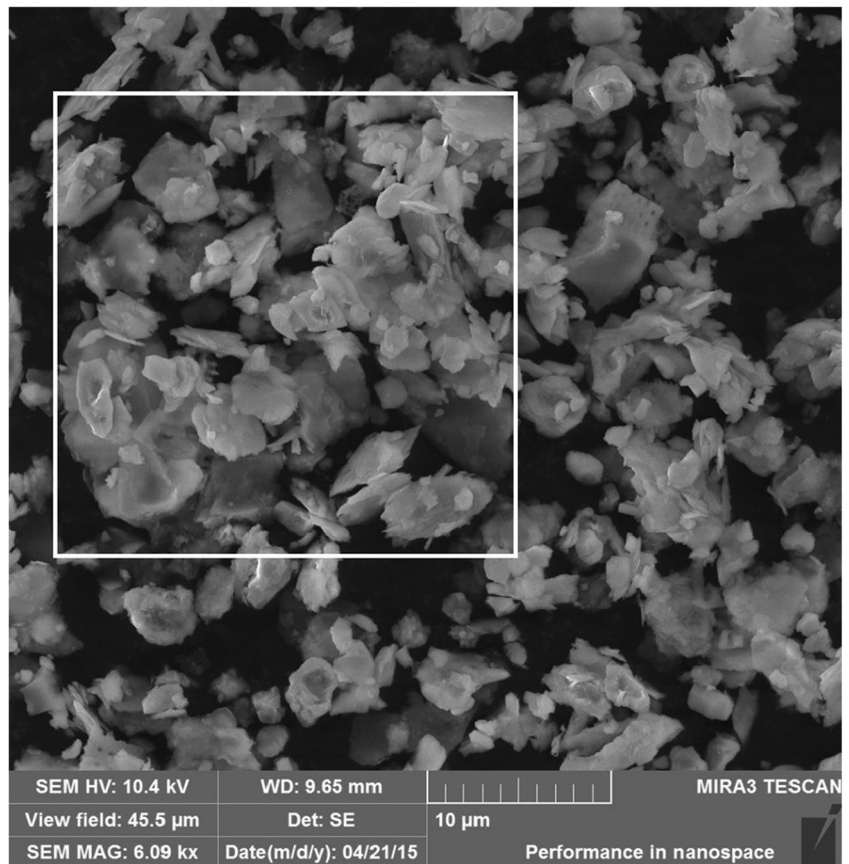
particle size interval between  $1 \mu\text{m}$  and  $2 \mu\text{m}$ , Stokes' law loses its validity. In the created colloidal dispersion, the movement of particles and their sedimentation rate is increasingly influenced by diffusion. It is evidenced by the development of sedimentation rates calculated by a modified Stokes' equation. The equation was modified by the correction factor  $K = 0.286$ . Stokes' equation (7) then has the following form:

$$u = \frac{2}{7} \frac{(\rho - \rho_0) \cdot r^2 \cdot g}{\eta_0} \tag{11}$$

**Fig. 6** Measured sedimentation rates and their comparison with the rates calculated by Stokes' equation (7) and (11)



**Fig. 7** Morphology of examined soil microparticles (Senné area), view fields 45.5

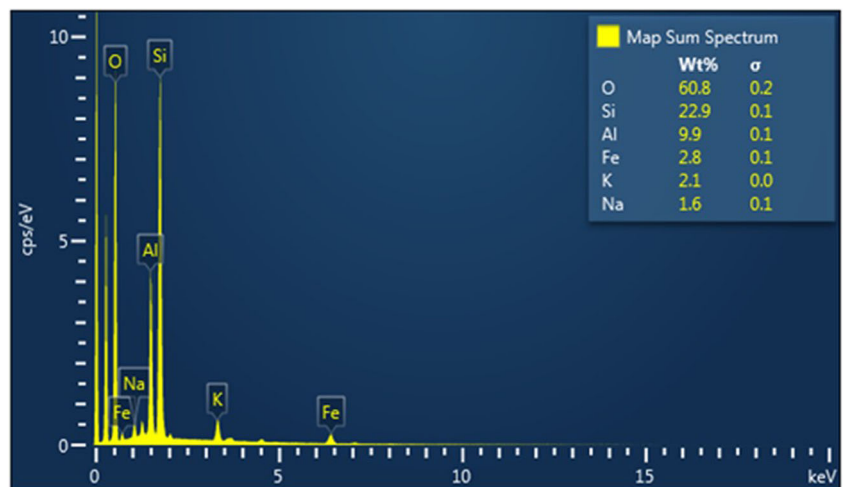


As mentioned before, the correction factor  $K$  depends on the particle size and also its shape. The shape of soil microparticles was examined by an electron microscope. The shape and size of the disperse phase, i.e. microparticles, are shown in Fig. 7. The pictures are the images from the electron microscope. Soil microparticles have the shape of a plate. The mean value of the width of the soil microparticles in Fig. 7 is around  $0.45 \mu\text{m}$ , the surface area is around  $1.58 \mu\text{m} \times 2.36 \mu\text{m}$ . The mean value of the particles volume is  $1.68 \mu\text{m}^3$ . Following

Eq. (9), it is represented by an equivalent spherical particle with the diameter  $d_e = 1.47 \mu\text{m}$ .

Figure 7 shows a field, in which the spectral analysis of the particle composition and the area distribution of the individual particles in the sample were performed. The spectral analysis results are shown in Fig. 8. From the summary spectrum map, the predominant elements in the studied samples are as follows: oxygen (60.2%), silicon (22.9%), and aluminium (9.9%). Together, it makes 93.6%. The remainder is iron,

**Fig. 8** Spectral analysis of elemental composition



potassium and sodium. In Fig. 9, the area distribution of the identified elements is illustrated. Their distribution corresponds to the distribution of the material in the sample. Figure 10 shows a dried deposit after the experiment. From this, it is possible to assess the optical properties of the material. The cross section is of matt white-gray colour. The scratch colour is white. Based on the information shown in Figs. 7, 8, 9 and 10, it can be assumed that the soil sample contains clay particles. In addition, volumetric changes of a soil sample of up to 40% (shrinkage) compared to the saturated state were observed in the examined site. In field conditions, during dry summer months, this results in the formation of a two-domain soil structure and the vertical movement of the soil surface. A crack porosity is created that significantly changes the hydraulic and hydrological properties of the soil environment. Consequently, it is possible to assume that a considerable part of clay minerals belongs to a montmorillonite group.

## Discussion

The authors of the paper assumed the existence of the lower limit of the Stokes law. They were based on the fact that with the reduction of the sedimented particle size, the movement of the particles will be reduced by diffusion until the state of the dynamic sedimentation equilibrium is reached. The beginning of this process was observed for particles with a diameter of about 2  $\mu\text{m}$ . In addition, soil microparticles have been found

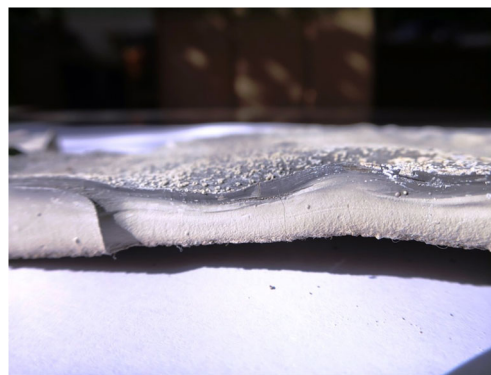
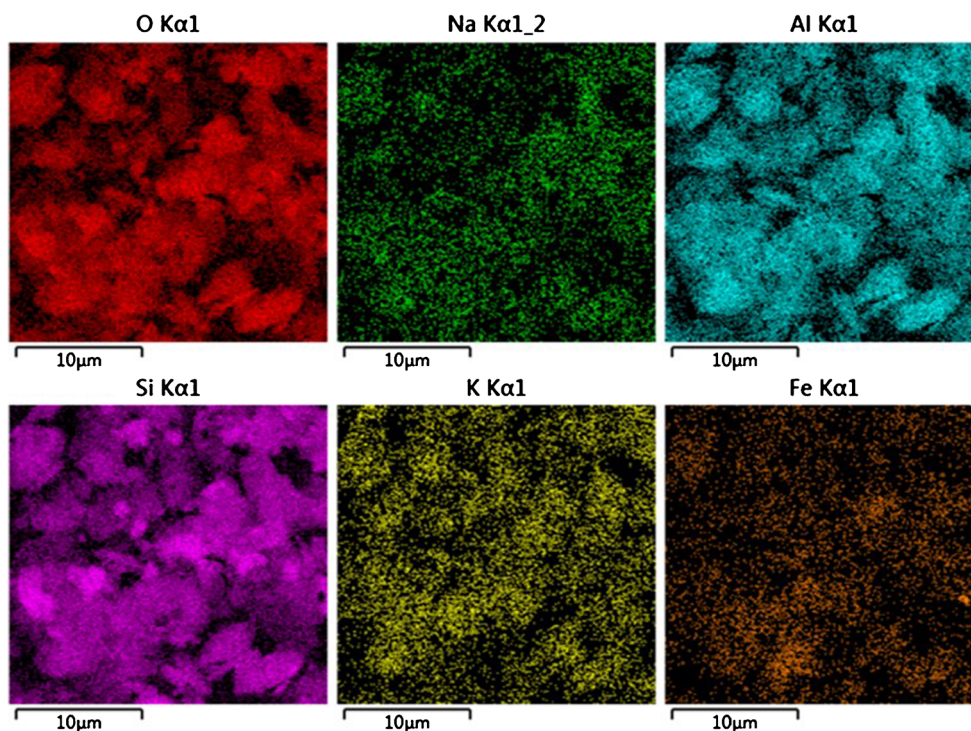


Fig. 10 Cross section of a dried sediment after the experiment

to have a plate-like shape that is roughly non-spherical. This, despite low speeds in the laminar flow area, can contribute to deviations from the rates following Stokes' relation. For the particles larger than 2  $\mu\text{m}$  (Fig. 6), it was found that Stokes' relation overstates the sedimentation rates compared to the rates which were actually measured. The main source of deviations will probably be the deviations from the spherical shape. The speed variations of the different particles are constant. For this reason, it is possible to modify Stokes' relation by a correction factor  $= \frac{2}{7}$ . The experiment shows that the laboratory procedures for soil texture analysis of clay soils based on the sedimentation are inappropriate. It is shown that when determining the content and rate of the sedimentation of particles sized  $> 2 \mu\text{m}$ , it is appropriate to calibrate the correction factor  $K$  in Stokes' relation in the individual geomorphological units.

Fig. 9 Surface distribution of identified elements in the investigated sample



## Conclusion

The aim of the experiment was to measure the sedimentation rate of different fractions of soil microparticles separated during the sedimentation, to define the lower validity limit for Stokes' equation, to illustrate the size and shape of soil microparticles and to quantify the influence of diffusion on sedimentation rate and formation of dynamic equilibrium of the created colloidal dispersion. Sedimentation analysis was selected as a method for particle size analysis. The disperse phase in the disperse system was represented by clay particles from the soil samples taken in the Senné area in the East Slovak Lowland (ESL). The dispersion medium was distilled water. Particle size analysis was performed by laser diffraction using the device Mastersizer 2000 (MALVERN Instruments). The speed of movement of the soil particles was measured based on the time and distance passed by particles with the diameter  $d(90)$ .

The results of the experiment showed that in laboratory conditions, Stokes' equation ceases to be valid for the sedimentation of the particles sized  $d(90) < 2 \mu\text{m}$ . For the sedimentation of the soil particles  $d(90) \in < 2; 10 > \mu\text{m}$  taken from the studied area, the correction factor  $K = 0.286$  was identified and Eq. (7) acquires the form (17). The particles smaller than this size create a colloidal dispersion. During the experiment, dynamic sedimentation equilibrium was reached at the particle size  $d(90) = 0.27 \mu\text{m}$ . The images of the particles showed that the particles are plate-shaped. The experiment shows that the laboratory procedures for soil texture analysis of clay soils based on sedimentation are inappropriate. It is shown that when determining the content and rate of the sedimentation of particles sized  $> 2 \mu\text{m}$ , it is appropriate to calibrate the correction factor  $K$  in Stokes' relation in the individual geomorphological units. The results of the experiment show that at constant temperature and viscosity, the shape and diffusion are critical for the rate deviations from Stokes' relation.

**Funding information** This contribution is the result of the implementation of the project: Centre of excellence for the integrated river basin management in the changing environmental conditions, ITMS code 26220120062, supported by the Research & Development Operational Programme funded by the ERDF. This study was supported by the Scientific Grant Agency of the Ministry of Education, Science, Research and Sport of the Slovak Republic (project VEGA: 2/0062/16, VEGA 1/0442/17).

## References

- Allain C, Cloitre M, Wafra M (1995) Aggregation and sedimentation in colloidal suspensions. *Phys Rev Lett* 74:1478–1481. <https://doi.org/10.1103/PhysRevLett.74.1478>
- Arkipov VA, Kozlov EA, Titov SS, Tkachenko AS, Usanina AS, Zharova IK (2016) Evolution of a liquid-drop aerosol cloud in the atmosphere. *Arab J Geosci* 9(114). <https://doi.org/10.1007/s12517-015-2161-4>
- Arriaga FJ, Lowery B, Mays MD (2006) A fast method for determining soil particle size distribution using a laser instrument. *Soil Sci* 171: 663–674. <https://doi.org/10.1097/01.ss.0000228056.92839.88>
- Bartovská L, Šišková M (2010) Fyzikální chemie povrchů a koloidních soustav. VŠCHT Praha
- Dellino P, Dioguardi F, Doronzo D M, Mele D (2018) The rate of sedimentation from turbulent suspension: an experimental model with application to pyroclastic density currents and discussion on the grain-size dependence of flow runout. *Sedimentology*, 0(ja).: <https://doi.org/10.1111/sed.12485>
- Durner W, Iden SC, von Unold G (2017) The integral suspension pressure method (ISP) for precise particle-size analysis by gravitational sedimentation. *Water Resour Res* 53:33–48. <https://doi.org/10.1002/2016WR019830>
- Everett DH (1988) Basic Principles of Colloid Science. In: Basic principles of colloid science. Royal Society of Chemistry, London
- Guan Y, Guadarrama-Lara R, Jia X, Zhang K (2017) Lattice Boltzmann simulation of flow past a non-spherical particle. *Adv Powder Technol* 28:1486–1494. <https://doi.org/10.1016/j.apt.2017.03.018>
- Haider A, Levenspiel O (1989) Drag coefficient and terminal velocity of spherical and nonspherical particles. *Powder Technol* 58:63–70. [https://doi.org/10.1016/0032-5910\(89\)80008-7](https://doi.org/10.1016/0032-5910(89)80008-7)
- Johnson T, Patel VC (1999) Flow past a sphere up to a Reynolds number of 300. *J Fluid Mech* 378:19–70. <https://doi.org/10.1017/S0022112098003206>
- Loizeau JL, Arbouille D, Santiago S, Vernet JP (1994) Evaluation of a wide range laser diffraction grain size analyzer for use with sediments. *Sedimentology* 41:353–361. <https://doi.org/10.1111/j.1365-3091.1994.tb01410.x>
- McRoberts EC, Nixon JF (1976) A theory of soil sedimentation. *Can Geotech J* 13:294–310. <https://doi.org/10.1139/t76-031>
- Miller BA, Schaetzl RJ (2012) Precision of soil particle size analysis using laser diffractometry. *Soil Sci Soc Am J* 76:1719–1727. <https://doi.org/10.2136/sssaj2011.0303>
- Moshrefi N (1993) A new method of sampling soil suspension for particle-size analysis. *Soil Sci* 155:245–248. <https://doi.org/10.1097/00010694-199304000-00002>
- Ouchene R, Khalij M, Taniere A, Arcen B (2015) Drag, lift and torque coefficients for ellipsoidal particles: from low to moderate particle Reynolds numbers. *Comput Fluids* 113:53–64. <https://doi.org/10.1016/j.compfluid.2014.12.005>
- Paul N, Biggs S, Shiels J, Hammond RB, Edmondson M, Maxwell L, Harbottle D, Hunter TN (2017) Influence of shape and surface charge on the sedimentation of spheroidal, cubic and rectangular cuboid particles. *Powder Technol* 322:75–83. <https://doi.org/10.1016/j.powtec.2017.09.002>
- Piazza R (2014) Settled and unsettled issues in particle settling. *Rep Prog Phys* 77:1–26. <https://doi.org/10.1088/0034-4885/77/5/056602>
- Richter A, Nikrityuk PA (2013) New correlations for heat and fluid flow past ellipsoidal and cubic particles at different angles of attack. *Powder Technol* 249:463–474. <https://doi.org/10.1016/j.powtec.2013.08.044>
- Rong LW, Zhou ZY, Yu AB (2015) Lattice-Boltzmann simulation of fluid flow through packed beds of uniform ellipsoids. *Powder Technol* 285:146–156. <https://doi.org/10.1016/j.powtec.2015.06.047>
- Sperazza M, Moore JN, Hendrix MS (2004) High-resolution particle size analysis of naturally occurring very fine-grained sediment through laser diffractometry. *J Sediment Res* 74:736–743. <https://doi.org/10.1306/031104740736>
- Stokes GG (1850) On the effect of the internal friction of fluids on the motion of pendulums. *Trans Cambridge Philos Soc* 9:8–106
- Storti F, Balsamo F (2010) Particle size distributions by laser diffraction: sensitivity of granular matter strength to analytical operating procedures. *Solid Earth* 1:25–48. <https://doi.org/10.5194/se-1-25-2010>

- Tan TS, Yong KY, Leong EC, Lee SL (1990) Sedimentation of clayed slurry. *Journal of geotechnical engineering*, vol 116. ASCE, pp 885–898. [https://doi.org/10.1061/\(ASCE\)0733-9410\(1990\)116:6\(885\)](https://doi.org/10.1061/(ASCE)0733-9410(1990)116:6(885))
- Taubner H, Roth B, Tippkötter R (2009) Determination of soil texture: comparison of the sedimentation method and the laser diffraction analysis. *J Plant Nutrition Soil Sci* 172:161–171. <https://doi.org/10.1002/jpln.200800085>
- Zaidi A, Tsuji T, Tanaka T (2014) A new relation of drag force for high Stokes number monodisperse spheres by direct numerical simulation. *Adv Powder Technol* 25:1860–1871. <https://doi.org/10.1016/j.apt.2014.07.019>
- Zhang N, Zhu W, Wang L, Lv YY, Zhou XZ (2013) Study of sedimentation and consolidation of soil particles in dredged slurry. *Rock Soil Mech* 34:1681–1686 [10.00-7598-\(2013\)06-1681-06](https://doi.org/10.00-7598-(2013)06-1681-06)
- Zhang N, Zhu W, He H, Lv Y (2017) Experimental study on sedimentation and consolidation of soil particles in dredged slurry. *J Civ Eng* 21:2596–2606. <https://doi.org/10.1007/s12205-017-0068-1>